Published in final edited form as:
Adv Funct Mater. 2013 February 5; 23(5): . doi:10.1002/adfm.201201945.

Endosomolytic anionic polymer for the cytoplasmic delivery of siRNAs in localized *in vivo* applications

Sariah Khormaee[1,2], **Yong Choi**[1], **Michael J. Shen**[1], **Biying Xu**[3], **Haitao Wu**[3], **Gary L. Griffiths**[3], **Rongjun Chen**[4], **Nigel K. H. Slater**[2], and **John K. Park**[1,*]

[1]Surgical and Molecular Neuro-oncology Unit, NINDS, NIH, Bethesda, MD, 20892, USA

[2]Department of Chemical Engineering and Biotechnology, University of Cambridge, Cambridge CB2 3RA, UK

[3]Imaging Probe Development Center, NHLBI, NIH, Rockville, MD, 20850, USA

[4]Centre for Molecular Nanoscience, School of Chemistry, University of Leeds, Leeds LS2 9JT, UK

Abstract

The use of small interfering RNAs (siRNAs) to down-regulate the expression of disease-associated proteins carries significant promise for the treatment of a variety of clinical disorders. One of the main barriers to the widespread clinical use of siRNAs, however, is their entrapment and degradation within the endolysosomal pathway of target cells. Here we report the trafficking and function of PP75, a non-toxic, biodegradable, lipid membrane disruptive anionic polymer composed of phenylalanine derivatized poly(L-lysine *iso*-phthalamide). PP75 is readily endocytosed by cells, safely permeabilizes endolysosomes in a pH dependent manner and facilitates the transfer of co-endocytosed materials directly into the cytoplasm. The covalent attachment of siRNAs to PP75 using disulfide linkages generates conjugates that effectively traffic siRNAs to the cytoplasm of target cells both *in vitro* and *in vivo*. In a subcutaneous malignant glioma tumor model, a locally delivered PP75-stathmin siRNA conjugate decreases stathmin expression in tumor cells and, in combination with the nitrosourea chemotherapy carmustine, is highly effective at inhibiting tumor growth. PP75 may be clinically useful for the local delivery of siRNAs, in particular for the treatment of solid tumors.

Keywords

siRNA delivery; anionic polymer; endosome; tumor treatment; glioblastoma; stathmin

1. Introduction

RNA interference (RNAi), the post-transcriptional silencing of target genes, can be triggered in mammalian cells by the intracytoplasmic delivery of synthetic siRNAs.[1, 2] Due to their relatively large size (~ 13 kDa) and high negative charge however, naked siRNAs cannot freely diffuse across cell membranes.[3] Virus-mediated RNAi, in which short hairpin RNAs (shRNAs) are transcribed and processed into siRNAs within transduced cells, is a highly efficient method of achieving targeted protein expression knockdown in experimental systems. For clinical purposes, however, enthusiasm for viral delivery systems is dampened by concerns regarding the elicitation of an anti-viral immune response and the random

*Corresponding author: John K. Park, 35 Convent Drive – MSC 3706, Building 35 – Room 2B-1002, Bethesda, MD, 20892, USA, voice: 301-402-6935; fax: 301-480-0099; parkjk@ninds.nih.gov.

integration of viral sequences into the host genome. Attention has therefore been focused on the development of safe and efficient non-viral siRNA delivery methods.

The three main classes of synthetic materials developed thus far for clinical siRNA delivery are: 1) liposomes and lipids, 2) cationic polymers and 3) siRNA conjugates.[3] Liposomes can be unilamellar or multilamellar with a nucleic acid payload core or they can be amorphous in structure with an interspersion of lipids and nucleic acids throughout. They have been shown to be effective at delivering both DNAs and siRNAs to cells, but there have also been concerns regarding their toxicity and the elicitation of off-target effects.[3, 4] Cationic polymers have the ability to bind and condense nucleic acids into stabilized nanoparticles that are readily endocytosed. Release of the nucleic acids into the cell cytosol, however, requires bursting of the enclosing endosomes. As a result, cationic polymers such as polyethyleneimine (PEI), the prototype for this class of delivery agent, are toxic at higher doses and can cause activation of the innate immune system.[5] Conjugation of siRNAs to membrane-permeant peptides and small molecules such as polyethylene glycol have also been used as a strategy to deliver siRNAs to cells, but overall toxicity has been an issue with this approach as well.[6, 7] It appears then that the entrapment of siRNAs within endolysosomal compartments and general toxicity are key barriers to the efficient delivery of siRNAs from the extracellular space to the cytoplasm.[4, 8] Non-toxic delivery vectors specifically designed to facilitate the release of siRNAs from endosomes would therefore be useful for the clinical implementation of RNAi-based treatment strategies.

Linear poly(L-lysine *iso*-phthalamide) backbone-derived anionic polymers demonstrate pH sensitive lytic behavior in lipid membrane experimental models. In high and neutral pH environments, the carboxylate groups contained within these polymers are deprotonated, and the repulsions among negative charges result in an extended polymer conformation. This extended conformation corresponds to the polymer in a lipid membrane neutral, non-disruptive state. In low pH environments, the carboxylate groups become protonated and hydrophobic interactions within the polymer backbone effect a transition to a compacted, lipid membrane disruptive state. The transition pH and lipid membrane disruption efficiency of the poly(L-lysine *iso*-phthalamide) backbone-derived polymers can be manipulated by chemically modifying the pendant carboxylate groups. One such modified polymer is PP75, which was derived by the grafting of L-phenylalanine onto the carboxylic acid moieties at a stoichiometric degree of substitution of 75 mol%. The actual degree of substitution of PP75, defined as the number of amino acid grafts per 100 carboxylic acid groups and determined by ^{1}H NMR in d_6-DMSO at room temperature, is 63.2%. The weight percentage (wt %) of amino acid grafts is 28.1% and the number average molecular weight (M_n) of PP75 as determined by MALDI-TOF is 22,720. PP75 was selected for characterization and development as an endosomal membrane lytic siRNA delivery vehicle because it has maximal lytic activity at pH 6.5, which is within the pH range characteristic of early endosomes (pH 6.0–6.8).[9]

We demonstrate here that PP75 is non-toxic and readily endocytosed by mammalian cells. It safely allows for the low pH-dependent release of co-endocytosed products into the cytoplasm and PP75-siRNA conjugates are effective at knocking down the expression of targeted proteins both *in vitro* and *in vivo*. Specifically, in a solid tumor experimental model, a PP75-siRNA conjugate directed against stathmin, a microtubule regulating protein that mediates resistance to nitrosoureas,[10] results in the knockdown of stathmin protein expression and increases sensitivity to drug treatment. These results indicate that PP75 is potentially useful for the local delivery of siRNAs in the clinical setting.

2. Results

2.1. PP75 undergoes clathrin-mediated endocytosis

PP75, an anionic polymer derived from the grafting of L-phenylalanine onto the pendant carboxylate groups of a poly(L-lysine *iso*-phthalamide) backbone (Fig. 1A) was selected for use as a potential endosomolytic siRNA delivery vehicle because it has maximal lytic activity within the pH range present in early endosomes.[9] To assess the ability of cells to safely initially uptake PP75, the polymer was conjugated to the fluorescent dye AlexaFluor 647. U251 malignant glioma cells readily take up the PP75-AF647 conjugate and this uptake can be quantitated using FACS analysis (Fig. 1B). Incubation of cells at 4°C, a temperature at which endocytosis is blocked, inhibits PP75-AF647 uptake and pre-treatment of cells with either hypertonic sucrose, which blocks clathrin-mediated endocytosis, or nystatin, which blocks caveolin-mediated endocytosis, decreases the internalization of PP75-AF647 by 65.7% and 12.2%, respectively (Fig. 1B). These results indicate that PP75 internalization can occur through either the clathrin- or caveolin- mediated endocytic pathways, but does so predominantly through the former. Further support for the preferential use of one pathway over the other is the differential co-localization of PP75-AF647 with transferrin and LacCer, ligands predominantly taken up by the clathrin- and caveolin- mediated endocytic pathways, respectively. The vast majority of PP75-AF647 (76.4%) co-localizes with transferrin. (Fig. 1C).

2.2. PP75 mediates pH dependent endosomolysis

The endosomolytic activity of PP75 in live cells was examined using the membrane impermeant fluorescent tracer calcein. Similar to siRNAs, calcein is non-specifically endocytosed by cells, but is unable to diffuse across the endosomal membrane.[13] As a consequence of this endosomal entrapment, its extracellular administration results in a punctate staining pattern within cells. When co-administered with PP75 however, calcein is diffusely present throughout the cytoplasm as a result of its release from endosomes (Fig. 2A). Consistent with the mechanism by which PP75 changes conformation and becomes lytic, the PP75-mediated release of calcein is dependent on endosomal acidification as demonstrated by the qualitative and quantitative blockage of diffuse cytoplasmic calcein staining in cells pre-treated with the endosomal acidification inhibitors BafA1 and ammonium chloride (NH_4Cl) (Fig. 2B). To restore the ability of NH_4Cl pre-treated cells to undergo endosomal acidification, the NH_4Cl was washed out one hour prior to the addition of calcein and PP75. This washout restores cytoplasmic calcein staining in PP75 treated cells (Fig. 2B).

Two possible mechanisms by which PP75 allows for the release of endosomal contents into the cytoplasm are rupture of the endosome and pore formation in the endosomal membrane. The circular staining pattern of PP75-AF647 seen in live cells using confocal microscopy strongly suggests that the endosomes have not ruptured and have largely maintained their circular shape (Fig. 2C). Further evidence for this is the identification of PP75-AF647 labeled circular structures that have equivalent calcein (green) fluorescence intensities inside and locally outside, reflecting the partial release of calcein from an intact but leaky endosome into the cytoplasm. PP75-AF647 stained ghost-like structures suggestive of ruptured endosomes are not seen. Given the likely escape of calcein from within endosomes into the cytoplasm through PP75-generated pores, we sought to determine if molecules similar or larger in size to siRNAs (~13 kDa) could also traverse the pores. TMR-dextran with molecular weights ranging from 3kD to as large as 70kD are readily released into the cytoplasm as demonstrated using confocal microscopy (Fig. 2D). These results demonstrate that PP75 can facilitate the release of endosomal contents similar or larger in size to siRNAs into the cytoplasm via the formation of pores in the endosomal membrane.

2.3. PP75 is non-toxic to cells

To address the possibility that calcein and TMR-dextrans may be entering the cytoplasm directly from the extracellular milieu secondary to direct or indirect PP75-mediated plasma membrane disruption, cells incubated with PP75 were assessed for plasma membrane integrity using lactate dehydrogenase (LDH) release and propidium iodide (PI) staining and for apoptosis using annexin V labeling and cytochrome c staining. LDH is a cytoplasmic enzyme that is rapidly released into the extracellular environment upon damage to the plasma membrane. Its presence in cell culture media can be detected as a result of its enzymatic activity. Cell populations incubated with PP75 do not demonstrate increased LDH release compared to vehicle controls (PBS) (Fig. 3A). PI is a plasma membrane impermeant dye that is generally excluded from cells with intact plasma membranes. FACS analysis demonstrates that cell populations incubated with PP75 likewise do not have increased uptake of PI when compared to controls (Fig. 3B). FACS analysis was also used to determine if PP75 induces cells to undergo apoptosis. During apoptosis, phosphatidyl serine translocates from the inner to the outer leaflet of the plasma membrane cells and this change can be detected using annexin V labeling. Treatment of cells with PP75 does not induce this apoptosis associated translocation (Fig. 3B). The release of cytochrome C from the mitochondria into the cytoplasm also occurs during apoptosis and staining of cells with anti-cytochrome C antibodies can assess this release. There does not appear to be any appreciable release of cytochrome C into the cytoplasms of cells following PP75 treatment (Fig. 3C). Taken together, these data provide support that PP75-mediated delivery of calcein and TMR-dextrans to the cytoplasm is unlikely to be occurring through a disrupted plasma membrane or as a result of polymer mediated apoptosis or cell death.

2.4. PP75 mediates *in vitro* and *in vivo* siRNA delivery

The efficacy of PP75 as an *in vitro* siRNA delivery vehicle was assessed using an siRNA against stathmin, a microtubule regulating protein previously shown to mediate chemoresistance in tumor cells.[10] Treatment of U251 malignant glioma cells with PP75 alone, stathmin siRNA alone or PP75 plus stathmin siRNA has no significant effects on stathmin mRNA and protein expression as determined by quantitative PCR (Fig. 4A) and immunoblotting with an anti-stathmin antibody (Fig. 4B), respectively. Given the proposed mechanism of action and physical properties of PP75, these results are not entirely unexpected. PP75 and the siRNAs requiring cytoplasmic delivery must necessarily be taken up and co-localized in the same endosome, but at the neutral pH of the tissue culture medium, both PP75 and siRNAs are negatively charged and likely subject to electrostatic repulsive forces. To ensure their initial co-uptake and subsequent separation once in the reducing environment of the maturing endolysosome, PP75 and siRNAs were conjugated via a disulfide bond. Cells treated with PP75-stathmin siRNA conjugate have 81% ($p < 0.002$; Student's t-test) and 90% reductions in stathmin mRNA and protein levels, respectively, compared to control untreated U251 cells. These decreased levels are also statistically significantly less than that seen in cells treated with PP75 alone, stathmin siRNA alone, PP75 plus stathmin siRNA stathmin without conjugation, and PP75 conjugated to a scrambled control siRNA (Figs. 4A and 4B).

Given the highly effective, gene-specific *in vitro* silencing activity of the PP75-siRNA complexes, we sought to confirm the presence of the siRNAs in the cytoplasm, their intracellular site of action. SiRNAs were 3′-labelled with the fluorescent dye Cy3 prior to their 5′-thiol conjugation to PP75. Treatment of U251 cells with the PP75-Cy3 labelled-siRNA conjugates results in the localization of Cy3-labelled siRNAs within the cytoplasm (Fig. 4C). As negative controls, Cy3-labelled siRNA alone, PP75 alone, and an unconjugated mixture of PP75 and Cy3-labelled siRNAs do not result in the cytoplasmic localization of Cy3-labelled siRNAs. As expected, the cytoplasmic delivery of polymer

conjugated siRNAs is siRNA sequence independent as PP75 conjugated -stathmin specific and -scrambled control Cy3-labelled siRNAs are both visible in the cytoplasm (Fig. 4C).

To assess their *in vivo* activity, PP75-stathmin siRNA conjugates were directly injected into U251 tumors subcutaneously established in the flanks of immunocompromised nude mice. Tumors were removed and assessed for stathmin mRNA levels using real time RT-PCR and protein levels using immunohistochemistry and immunoblotting. There is a 60% reduction in stathmin mRNA in PP75-stathmin siRNA injected tumors compared to control tumors injected with PP75 alone ($p<0.005$; Student's t-test). PP75-stathmin siRNA injected tumors also have significantly less stathmin mRNA when compared to control tumors injected with stathmin siRNA alone or PP75-scrambled siRNA conjugates ($p<0.005$; Student's t-test) (Fig. 5A). Likewise, there is an approximately 50% decrease in stathmin protein expression in PP75-stathmin siRNA injected tumors compared to all control injected tumors as determined by immunoblotting (Fig. 5B) and a corresponding qualitative decrease as determined by immunohistochemistry (Fig. 5C).

2.5. PP75-stathmin siRNA conjugates inhibit tumor growth *in vivo*

To determine the efficacy of the PP75-stathmin siRNA conjugates in a tumor treatment model, nude mice with subcutaneous U251 tumors were treated intraperitoneally with carmustine, a nitrosourea chemotherapeutic agent, as well as intratumorally with PP75-stathmin siRNA conjugate, PP75-scrambled siRNA conjugate, PP75 alone or stathmin siRNA alone, the latter three again serving as negative controls. We have previously demonstrated that lentivirus-mediated stathmin knockdown sensitizes tumors to carmustine.[10] The combination of carmustine and PP75-stathmin siRNA conjugates significantly increases the sensitivity of tumors to carmustine. Tumor sizes of animals in this treatment group are significantly smaller than that of animals in each of the three control groups ($p < 0.001$; two-way ANOVA) while tumor sizes of animals in each of the three control groups do not significantly differ from each other ($p > 0.05$; two-way ANOVA) (Fig. 5D).

It has been shown that siRNAs can elicit an innate immune response in a sequence dependent manner.[14] To rule out the possibility that PP75-stathmin siRNA conjugates inhibit tumor growth by preferentially eliciting such a response, we examined PP75-stathmin siRNA and PP75-scrambled siRNA treated tumors for the presence of monocytes/macrophages, dendritic cells and NK cells. Staining of tissue sections with antibodies against CD11b, a phenotypic marker for these cells, reveals that neither conjugate elicits an innate immune response to any appreciable degree (Figs. 6A and 6B). Given the use of nude mice as tumor hosts, the infiltration of tumors by adaptive immune response cells is not possible.

3.0. Discussion and Conclusions

Early clinical studies have shown that siRNAs hold tremendous promise as therapeutic agents due to their exquisite ability to selectively silence the expression of pathologic genes.[15–18] One of the main barriers to the widespread clinical use of siRNAs, however, is the lack of delivery agents that can efficiently deliver them to their cellular site of action, the cytoplasm.[4] To address this challenge, we conjugated siRNAs to PP75, an anionic polymer that is readily endocytosed by cells and subsequently causes the pH-dependent disruption of enclosing endosomes. The *in vitro* and *in vivo* knockdowns of stathmin mRNA and protein levels by PP75-stathmin siRNA conjugates are demonstration of the efficacy of PP75 as an siRNA delivery vehicle. Furthermore, PP75-stathmin siRNA conjugates increase the sensitivity of tumors to carmustine, an effect previously seen using lentivirus-mediated stathmin shRNA delivery.[10, 19]

The physical properties of PP75 offer a number of advantages over previously developed siRNA delivery agents. Due to its negative charge, PP75 is less likely to be inactivated by binding to negatively charged serum proteins and less likely to cause protein aggregation *in vivo* as can be seen with cationic agents.[3, 20] While repulsion to negatively charged cell membranes is a theoretical obstacle to the cellular uptake of PP75-siRNA complexes, the complexes were readily endocytosed, predominantly via the clathrin-mediated pathway. Another theoretical disadvantage to the use of an anionic delivery agent is its inability to form spontaneous complexes with siRNAs as cationic agents can do. A simple disulfide linkage is, however, not only sufficient to ensure their co-uptake by cells, but also likely allows for separation of the siRNA and the polymer in the reducing environment of the acidifying endosome.

While overall toxicity has hampered the widespread use of many siRNA delivery agents, PP75 does not appear to suffer this limitation. Previous work by our group has shown that concentrations as high as 4 mg/mL are non-toxic to cells *in vitro*.[21] In our current studies, PP75-stathmin siRNA complexes at a concentration of 0.5 mg/L are effective at inhibiting stathmin expression without inducing plasma membrane damage, apoptosis or an appreciable innate immune response. Because previous studies have shown that the interstitial pH within tumors decreases as the distance from the closest blood vessel increases, another theoretical toxicity concern regarding the *in vivo* use of a compound that is lipid membrane lytic in low pH environments is non-specific damage to the plasma membrane of non-neoplastic cells within the acidotic environment of a solid tumor. Such non-specific plasma membrane damage is, however, unlikely because the interstitial pH of tumors plateaus at a low of approximately 6.7 while PP75 undergoes transition from a membrane-neutral to a membrane–disruptive state at a pH of approximately 6.1.[22,12]

Recent studies have reported the design and synthesis of multifunctional nanoparticles, multicomponent polymer systems, and delivery vectors based upon viral cell penetrating peptides for the more efficient delivery of siRNAs to target cells.[15,23–25] In contrast, PP75 is a simple-structured anionic polymer that is easily synthesized, non-toxic and effective *in vivo*. PP75 can be readily conjugated to siRNAs via a disulfide linkage that not only ensures their co-uptake by cells, but also allows for the subsequent separation of the two components in the reducing environment of the acidifying endosome. The significance of our results is that this is the first report, to our knowledge, of an anionic polymeric siRNA delivery vehicle that has demonstrable efficacy in an *in vivo* disease model.

In summary, anionic polymers with endosomolytic activity are an innovative and promising new class of non-toxic, biodegradable vehicles for the safe and efficient *in vivo* delivery of siRNAs to the cytoplasm of target cells. PP75, a prototype of this class, is well suited for local delivery applications such as that required for the induction of RNA interference in solid organs or tumors.

4.0. Experimental

Materials

All polymer synthesis materials were reagent grade. Coupling agents 1-ethyl-3-(3-dimethylaminopropyl)carbodiimide hydrochloride (EDC) and N-hydroxysulfosuccinimide (Sulfo-NHS) were obtained from Fisher Scientific (Fair Lawn, NJ). N-Succinimidyl 3-(2-pyridyldithio)-propionate (SPDP) was obtained from Pierce Chemical (Rockford, IL). All other polymer synthesis materials, calcein and endocytosis inhibitors were obtained from Sigma Aldrich (St. Louis, MO). Alexa Fluor 647 cadaverine (AF647 cadaverine), tetramethylrhodamine labeled dextrans (TMR-dextran) and Alexa Fluor 488 transferrin (transferrin-AF488) were obtained from Invitrogen (Carlsbad, CA). Thiol-5′ ± Cy3-3′

modified sense RNA nucleotides for stathmin (5′-GUGCGGAAGAACAAAGAAUTT-3′) and a scrambled control (5′-AAAGUACGGAAGACGAAGATT-3′), as well as the respective corresponding unmodified anti-sense RNA nucleotides, were obtained from Integrated DNA Technologies (Coralville, Iowa). Cell culture media and reagents were purchased from Mediatech (Herndon, VA). U251 cells were purchased from American type Culture Collection (Manassas, VA). Cell culture chamber slides were purchased from Lab-Tech of VWR (Fair Lawn, NJ).

Cell culture

U251 human malignant glioma cells (ATCC, Manassas, VA) were maintained in Dulbecco's Modified Eagle's Medium (DMEM) supplemented with fetal bovine serum (10%), penicillin (100 μg/mL) and streptomycin (100 IU/mL). Cells were passaged biweekly with trypsin/EDTA and maintained at 37°C humidified 5% CO2 incubator.

Polymer conjugation to AF647

Phenylalanine grafted poly(L-lysine iso-phthalamide) (PP75) was synthesized as previously described in detail. [9, 11, 12] PP75 and AF647-cadaverine were conjugated via aqueous EDC/sulfo-NHS coupling using the following reaction sequence. PP75 (10mg, 20 eq. COOH) was dissolved in DMSO (900 μL) and HPLC grade water (50 μL). EDC (10.4 mg, 40 eq.) and sulfo-NHS (23.5 mg, 80 eq.) were dissolved together in water (75 μL) and then added to the PP75 solution in order to activate the carboxyl groups of PP75. After allowing this activation reaction to proceed for 1 h at room temperature, AF647-cadaverine (1.5 mg, 1 eq.) dissolved in sodium carbonate (pH = 9, 500 μL, 1 M) was added, and reacted overnight in the dark at room temperature (Fig. S1). The resulting product was dialyzed against water and lyophilized to yield a blue powder. Formation of the PP75 conjugated AF647 (PP75-AF647) was verified by HPLC analysis with a Zorbax PSM-60 column on an Agilent 110 HPLC system with 10% DMSO/water as a mobile phase and flow rate of 1 mL/min (Figs. S2A–D).

Polymer conjugation to siRNA

PP75 was conjugated via disulfide linkage to 5′ sulfhydryl modified siRNAs using the following reaction sequence. SPDP-cadaverine linker was first synthesized by adding N-Boc-1,5-diaminopentane (0.05 mmol) to SPDP (0.05 mmol) dissolved in acetonitrile (0.5 mL). The mixture was shaken at room temperature and lyophilized to yield a white powder. To remove the Boc protecting groups, TFA was added to this product for 1 h and then evaporated (Fig. S3A). The remaining product was dissolved in acetonitrile (1 mL) and loaded onto a Zorbax XDB C18 column (9.8 × 250 mm, 5μm). The column was eluted using a 30% to 95% gradient of 0.05% TFA/acetonitrile in 0.05% TFA/water at a flow rate of 4 mL/min (Fig. S3B). The eluted product was again lyophilized to afford a white solid and analyzed by proton NMR (Fig. S3C) and MS (Fig. S3D) to confirm the synthesis of SPDP-cadaverine. SPDP-cadaverine linker was added to 5′ sulfhydryl modified siRNAs using the following reaction sequence (Fig. S4A). The siRNAs were suspended in Tris-EDTA to yield 100uM solutions and the corresponding sense and anti-sense strands were annealed by heating to 90°C for 5min and then cooling to RT. A 100 fold molar excess of TCEP (50 μL of 5 mg/mL) was added to the siRNA and allowed to incubate at room temperature for 90 min to free the sulfhydryl groups of the siRNA. Reduction of the disulfide bonds was verified by MALDI and the siRNA/TCEP (20 μL) mixture was reacted with SPDP-cadaverine (1.5 mg dissolved in 40 μL of water) mixed with DMS0 (50/50 by volume). The reaction was monitored via MALDI and allowed to proceed for 30 min at room temperature (Fig. S4B). The SPDP-cadaverine siRNA product was then desalted and buffer exchanged to carbonate buffer (0.1 M) with a NAP-5 column, and further concentrated with YM-3 spin tubes. The final conjugation of PP75 to siRNA was carried out using the following reaction

sequence (Fig. S5A). PP75 (1 mg) dissolved in DMSO/MES buffer containing EDC (1.1 mg) and sulfo-NHS (2.4 mg) was mixed with SPDP-cadaverine siRNA (300 μg) and the coupling reaction was allowed to proceed at room temperature for 4 h and then overnight at 4°C. The conjugation reaction was verified using HPLC (Fig. S5B–E). PP75-siRNA conjugates were purified by size exclusion chromatography with a G3000PW column (Tosoh Bioscience, Stuttgart, Germany).

Calcein and TMR-dextran staining of cells

U251 cells maintained as described above were seeded in 24 well cell culture plates (Corning, Corning, NY), at a density of 3×10^4 cells/well. After two days in culture, cells were treated with calcein (2 mg/mL) or TMR-dextran (2 mg/mL) for 30 minutes and then washed three times with Dulbecco's PBS (Mediatech). PP75 (0.5 mg/L), where indicated, was added for 30 mins at either 37° or 4°C. For cells incubated at 4°C, a 5 min preincubation step was used to allow cells to reach the new lower temperature prior to introduction of polymer and calcein. Cells were imaged using a Zeiss LSM 501 confocal microscope outfitted with a heated stage blower (Carl Zeiss, Inc., Jena, Germany). For inhibition of endosomal acidification, either bafilomycin A1 (BafA1, 1 nM, Sigma Aldrich) or NH_4Cl (50 mM, Sigma Aldrich) in additive-free DMEM (0.5 mL) was added to cells 20 minutes prior to the addition of calcein and/or PP75. In order to remove NH_4Cl and re-acidify endosomes prior to calcein addition, two 10 min and one 40 min washes with DMEM were performed.

Cellular uptake of PP75-AF647

U251 cells were seeded as described above. After two days in culture, the media was removed and replaced with additive free DMEM containing either sucrose (0.3 M) to inhibit clathrin mediated endocytosis or nystatin (25 μg/mL, Sigma Aldrich) to inhibit caveolin mediated endocytosis. Cells were incubated with inhibitors for 30 min prior to addition of PP75-AF647 (2 mg/mL). After a further 30 min incubation, polymer and inhibitors were aspirated. Cells were subsequently washed with Trypan Blue (0.4%) to quench extracellular AF647 fluorescence and then rinsed four times with PBS. For fluorescent assisted cell sorting (FACS) analysis, cells were trypsinized, pelleted by centrifugation (120 g for 5 min), and analyzed using a FACS Calibur system outfitted with a 644 nm Red-diode laser (BD Biosciences, San Jose, CA). 5000 cells were analyzed for each experimental condition using FACS Calibur Software (BD Biosciences) and all experiments were carried out in triplicate. For the co-localization of endosomal tracers with PP75, U251 cells were seeded as described above. After 2 days in culture, the media was removed and replaced with additive free DMEM (0.5 mL) containing PP75-AF647 (2 mg/mL) and either transferrin-AF648 (20 mg/mL) or LacCer-BODIPY (2 μM). Cells were allowed to internalize the compounds for 30 min, after which time, the media was aspirated and wells were treated with Trypan Blue to quench extracellular fluorescence, as described above. Cells were imaged immediately using a confocal microscope.

In vitro and in vivo siRNA delivery

U251 cells were seeded as described above. After 2 days in culture, the media was removed and replaced with additive free DMEM (0.5 mL) containing vehicle, PP75 (0.5 mg/L) alone, stathmin siRNA (200 ng/mL; 15 nM) alone, PP75 plus stathmin siRNA without conjugation (0.5 mg/L of polymer; 200 ng/mL of siRNA), PP75-stathmin siRNA conjugates (0.5 mg/L of polymer – 200 ng/mL of siRNA), PP75-scrambled siRNA conjugates (0.5 mg/L of polymer – 200 ng/mL of siRNA) or stathmin siRNA (200 ng/mL) plus Lipofectamine (Invitrogen) according to manufacturer's directions. Two days later, the cells were subjected to real time RT-PCR and immunoblot analysis of stathmin expression as described below. Cells were also assessed for viability and the induction of apoptosis as described below. For

in vivo delivery experiments, subcutaneous tumors were established by injecting U251 cells (5×10^6) into the left dorsum of 6 to 8 week-old nude mice (BALB/cAnNCr-nu/nu; NCI-Frederick, Frederick, MD). After 5 days, mice bearing tumors greater than 10 mm^3 (n = 28 total mice) were randomly divided into four groups and received intratumoral injections (0.2 mL) of PP75 (0.5 mg/L), stathmin siRNA (15 nM), PP75-stathmin siRNA (0.5 mg/L) or PP75-scrambled siRNA (0.5 mg/L) on two consecutive days. Two days thereafter, three animals from each group were randomly selected and euthanized. Tumors from these selected animals were assessed for stathmin mRNA expression using real time RT-PCR and protein levels using immunoblot and immunohistochemistry as described below. The remaining animals were treated with intraperitoneal administration of 1,3-bis(2-chloroethyl)-1-nitrosourea (BCNU; 15 mg/kg, Bristol-Myers Squibb; New York, NY) in 10% ethanol (Sigma). Serial tumor measurements were carried out using a digital caliper every three to four days and tumor volumes (V) were calculated using the formula: V = 0.5 × length × width. For statistical analysis of tumor volumes, two-way ANOVA was performed using GraphPad Prism version 5.03 for Windows (GraphPad Software, San Diego, CA). All procedures were in accordance with NIH Animal Care and Use Committee protocols.

Cell viability and apoptosis analyses

The CytoTox 96 kit (Promega Corp., Madison, WI) was used to assess the plasma membrane integrity and viability of cells treated with PP75. U251 cells were grown to 60% confluency and treated with PBS control, PP75 or actinomycin D (ActD; Sigma-Aldrich) treatment (100 ng/mL) as a positive control. After 48 hr, 50 μL of the cell growth media was removed from each sample and assayed for lactate dehydrogenase (LDH) according to the manufacturer's instructions. Colorimetric measurements were performed using a SpectraMax® Plus 384 Microplate Spectrophotometer (Molecular Devices Corporation, Sunnyvale, CA). Media from lysis buffer treated cells were used to determine maximal release values. Experiments were performed in quadruplicate. For propidium iodide (PI) and annexin V labeling, U251 cells were treated with PBS control, PP75 or ActD as described above. After 48 hours of treatment, the cells were trypsinized, washed and stained with PI and annexin V (both Trevinogen, Gaithersburg, MD) according to the manufacturer's directions. PI staining and annexin V binding were analyzed by FACS utilizing a Becton Dickinson FACSCalibur and Cell Quest software. Experiments were performed in triplicate. For the assessment of mitochondrial cytochrome c release, U251 cells were plated in four-well chamber slides (Nalge Nunc International, Naperville, IL), and treated with PBS control, PP75 or ActD in the presence of the caspase inhibitor Q-VD-OPH (QVD, SM Biochemicals, Anaheim, CA) (40 μM) for 48hr. At the end of treatment, cells were washed twice with PBS and fixed with 4% paraformaldehyde for 15 min at room temperature. Fixed cells were washed twice with PBS and incubated in blocking buffer (3% BSA and 0.3% Triton-X in PBS) for 30 min at room temperature. Cells were then incubated for 1 hr at room temperature with anti-cytochrome c antibody (BD Biosciences) (1:500), washed three times with PBS, and incubated with Alexa-Fluor 546 goat anti-mouse secondary antibody (Invitrogen) 30 min at room temperature. After washing five times with PBS, cells were mounted in ProLong Gold Antifade reagent with DAPI. Images were captured using a confocal microscope.

Immunoblot Analysis

Proteins extracted from cells and tissues were resolved by SDS-PAGE and transferred to polyvinylidene difluoride membranes (Millipore, Billerica, MA). Membranes were probed with rabbit anti-stathmin (EMD Chemicals, Gibbstown, NJ) and mouse anti–β-actin (Sigma-Aldrich) antibodies, washed and reprobed with alkaline phosphatase–conjugated goat anti-rabbit IgG (Jackson Laboratory, Bar Harbor, ME) and alkaline phosphatase–conjugated goat

anti-rabbit IgG (Sigma-Aldrich) antibodies. Membranes were developed using 9H-(1,3-dichloro-9,9-dimethylacridin-2-one-7-yl) phosphate (DDAO phosphate, Invitrogen) and scanned using an FLA-5100 laser based scanner (Fujifilm, Stamford, CT). Quantitation of protein signals was performed using MultiGauge software (Fujifilm).

Quantitative real-time reverse transcription PCR

Total RNA was extracted from cultured U251 cells using the RNeasy Mini Column (Qiagen, Valencia, CA) or from tumor tissues using TRIzol ® reagent (Invitrogen). The RNA was treated with DNase I (Invitrogen) to eliminate traces of genomic DNA and cDNAs were synthesized using SuperScript III Reverse Transcriptase (Invitrogen) and random primers (Invitrogen). All procedures were done according to the manufacturer's protocols. Quantitative PCR was carried out using real time TaqMan™ technology in the Prism 7900HT sequence detection system with sequence-specific primers and probes (stathmin1 [Hs01027516_g1] and 18s rRNA [Hs99999901_s1]) (Applied Biosystems, Carlsbad, CA). A cycle threshold value in the linear range of amplification was selected for each sample and normalized for level of 18S rRNA expression. The relative stathmin expression level of each sample was calculated using the formula $2^{-\Delta\Delta CT}$, where $\Delta\Delta CT$ is the difference between the selected cycle threshold value of a particular sample and the mean of the cycle thresholds of the non-treated cells or tumor tissues. The experiments were repeated in triplicate, and the mean value with standard deviation is reported. Statistical analysis was performed using GraphPad Prism version 5.03 for Windows.

Immunohistochemistry

Tumor specimens were removed from animals, fixed in paraformaldehyde, embedded in paraffin, sectioned with a microtome, and mounted on glass slides. Sections were deparaffinized in xylene, washed in ethanol, and subjected to heat-induced antigen retrieval in sodium citrate buffer (pH 6.0) and Tween-20 (0.05%) for 25 min. Sections were blocked and permeabilized in blocking buffer (PBS, 5% normal donkey serum, 0.05% Triton X-100) for 1h at room temperature, and incubated with goat anti-stathmin antibodies (1:50 dilution; Santa Cruz Biotechnology, Santa Cruz, CA) and or Alexa Fluor 488 mouse anti-human CD11/Mac-1 monoclonal antibodies (1:250; Invitrogen) at 4°C overnight. Sections were washed and anti-stathmin stained sections were incubated with Alexa Fluor 594-conjugated chicken anti-goat IgG (1:500 dilution; Invitrogen) for 1hr at room temperature and washed again. All sections were mounted with ProLong Gold Antifade reagent with DAPI (Invitrogen). Images were taken with a confocal microscope.

Supplementary Material

Refer to Web version on PubMed Central for supplementary material.

Acknowledgments

This work was supported by the NINDS and NHLBI intramural research programs of the NIH and the NIH/Marshall fund. The Imaging Probe Development Center is supported by the NIH Roadmap for Medical Research Initiative of the NIH. We thank Dragan Maric for assistance with FACS analyses and Carolyn Smith for assistance with microscopy. There are no conflicts of interest to report. Supporting Information is available online from Wiley InterScience or from the author.

References

1. Fire A, Xu S, Montgomery MK, Kostas SA, Driver SE, Mello CC. Nature. 1998; 391:806. [PubMed: 9486653]

2. Elbashir SM, Harborth J, Lendeckel W, Yalcin A, Weber K, Tuschl T. Nature. 2001; 411:494. [PubMed: 11373684]
3. Whitehead KA, Langer R, Anderson DG. Nat Rev Drug Discov. 2009; 8:129. [PubMed: 19180106]
4. Petrocca F, Lieberman J. J Clin Oncol. 2011; 29:747. [PubMed: 21079135]
5. Kircheis R, Wightman L, Wagner E. Adv Drug Deliv Rev. 2001; 53:341. [PubMed: 11744176]
6. Muratovska A, Eccles MR. FEBS Lett. 2004; 558:63. [PubMed: 14759517]
7. Oishi M, Nagasaki Y, Itaka K, Nishiyama N, Kataoka K. J Am Chem Soc. 2005; 127:1624. [PubMed: 15700981]
8. Akhtar S, Benter IF. J Clin Invest. 2007; 117:3623. [PubMed: 18060020]
9. Chen R, Khormaee S, Eccleston ME, Slater NK. Biomaterials. 2009; 30:1954. [PubMed: 19138797]
10. Ngo TT, Peng T, Liang XJ, Akeju O, Pastorino S, Zhang W, Kotliarov Y, Zenklusen JC, Fine HA, Maric D, Wen PY, De Girolami U, Black PM, Wu WW, Shen RF, Jeffries NO, Kang DW, Park JK. J Natl Cancer Inst. 2007; 99:639. [PubMed: 17440165]
11. Eccleston ME, Kuiper M, Gilchrist FM, Slater NK. J Control Release. 2000; 69:297. [PubMed: 11064136]
12. Khormaee S, Chen R, Park JK, Slater NK. J Biomater Sci Polym Ed. 2010; 21:1573. [PubMed: 20537242]
13. Jones RA, Cheung CY, Black FE, Zia JK, Stayton PS, Hoffman AS, Wilson MR. Biochem J. 2003; 372:65. [PubMed: 12583812]
14. Judge AD, Sood V, Shaw JR, Fang D, McClintock K, MacLachlan I. Nat Biotechnol. 2005; 23:457. [PubMed: 15778705]
15. Davis ME, Zuckerman JE, Choi CH, Seligson D, Tolcher A, Alabi CA, Yen Y, Heidel JD, Ribas A. Nature. 2010; 464:1067. [PubMed: 20305636]
16. DeVincenzo J, Lambkin-Williams R, Wilkinson T, Cehelsky J, Nochur S, Walsh E, Meyers R, Gollob J, Vaishnaw A. Proc Natl Acad Sci U S A. 2010; 107:8800. [PubMed: 20421463]
17. Kaiser PK, Symons RC, Shah SM, Quinlan EJ, Tabandeh H, Do DV, Reisen G, Lockridge JA, Short B, Guerciolini R, Nguyen QD. Am J Ophthalmol. 2010; 150:33. [PubMed: 20609706]
18. Leachman SA, Hickerson RP, Schwartz ME, Bullough EE, Hutcherson SL, Boucher KM, Hansen CD, Eliason MJ, Srivatsa GS, Kornbrust DJ, Smith FJ, McLean WI, Milstone LM, Kaspar RL. Mol Ther. 2010; 18:442. [PubMed: 19935778]
19. Liang XJ, Choi Y, Sackett DL, Park JK. Cancer Res. 2008; 68:5267. [PubMed: 18593927]
20. Grayson AC, Doody AM, Putnam D. Pharm Res. 2006; 23:1868. [PubMed: 16845585]
21. Ho VH, Slater NK, Chen R. Biomaterials. 2011; 32:2953. [PubMed: 21272931]
22. Helmlinger G, Yuan F, Dellian M, Jain RK. Nat Med. 1997; 3:177. [PubMed: 9018236]
23. Convertine AJ, Benoit DS, Duvall CL, Hoffman AS, Stayton PS. J Control Release. 2009; 133:221. [PubMed: 18973780]
24. Rozema DB, Lewis DL, Wakefield DH, Wong SC, Klein JJ, Roesch PL, Bertin SL, Reppen TW, Chu Q, Blokhin AV, Hagstrom JE, Wolff JA. Proc Natl Acad Sci U S A. 2007; 104:12982. [PubMed: 17652171]
25. Endoh T, Ohtsuki T. Adv Drug Deliv Rev. 2009; 61:704. [PubMed: 19383521]

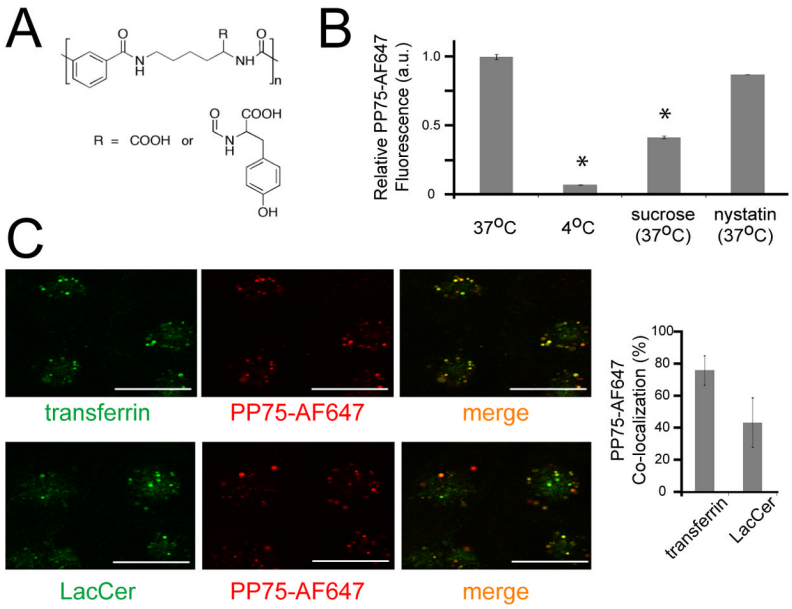

Fig. 1. Structure and cellular uptake of PP75

(**A**) Chemical structure of PP75 where the ratio between carboxylate and phenylalanine on the side chain R is 37:63. (**B**) FACS analysis was used to quantitate the relative uptake of fluorescently labeled PP75 (PP75-AF647) by U251 cells. Cells were treated with PP75-AF647 alone at 37°C or at 4°C. Cells were also treated with PP75-AF647 in combination with sucrose, a clathrin-mediated endocytosis inhibitor, or nystatin, a caveolin-mediated endocytosis inhibitor (both at 37°C). The mean fluorescence intensity values were normalized to that of cells treated with PP75-AF647 alone at 37°C. Error bars represent the standard deviation of triplicate experiments. The results indicate that PP75-AF647 is predominantly taken up by cells via clathrin-mediated endocytosis. (**C**) Cells were incubated with PP75-AF648 (red fluorescence) and either transferrin-AF488 (green fluorescence), a clathrin endocytosis marker, or BODIPY-LacCer (green fluorescence), a caveolin endocytosis marker, and visualized using confocal fluorescence microscopy. Overlay of the red and green channels reveals areas of co-localization (yellow fluorescence) and quantitation of this co-localization was performed using MetaMorph software. The mean percentage overlap of PP75-AF647 with transferrin-AF488 or BODIPY-LacCer is shown to the right of the microscopy images and error bars represent the standard deviation of triplicate experiments. Scale bars in the photos represent 20 μm. The greater overlap of PP75-AF647 with transferrin-AF488 supports the preferential uptake of PP75 via clathrin-mediated endocytosis compared to caveolin-mediated endocytosis.

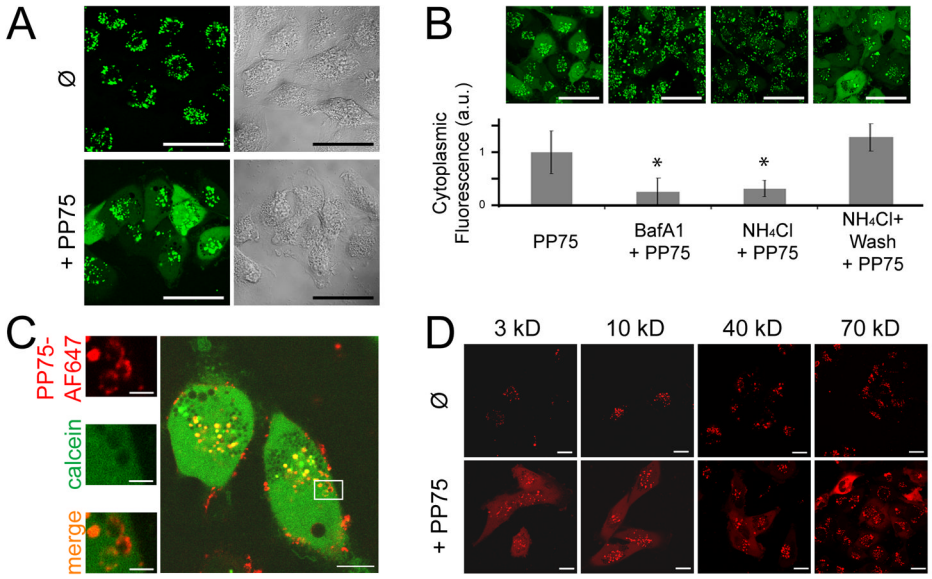

Fig. 2. PP75 trafficking and pore formation in endosomes

(**A**) U251 cells were incubated with the green fluorescent dye calcein in the absence (Ø) or presence (+PP75) of PP75 for 30 min. Confocal fluorescence microscopy images are shown on the left and the corresponding transmitted light images are shown on the right. Only in the presence of PP75 is there endoplasmic release and subsequent cytoplasmic localization of calcein as indicted by the diffuse green staining pattern. Scale bars represent 50 μm. (**B**) U251 cells were treated with the endosomal acidification inhibitors BafA1 or ammonium chloride (NH_4Cl) prior to incubation with calcein and PP75. Representative confocal fluorescence microscopy images shown across the top indicate that inhibition of endosomal acidification inhibits cytoplasmic calcein staining. Restoration of endosomal acidification activity in NH_4Cl pre-treated cells by washout of NH_4Cl one hour prior to incubation with calcein and PP75 restores cytoplasmic calcein staining. Scale bars represent 50 μm. Below each microscopy image is the relative cytoplasmic fluorescence intensity in arbitrary units (a.u.) of correspondingly treated cells. For each condition, 160 randomly selected cells were analyzed and a mean value was calculated. Asterisks indicate $p < 0.05$ in comparison to calcein + PP75 alone (PP75) (student's t test). (**C**) Cells were treated with calcein (green fluorescence) and PP75-AF647 (red fluorescence). Calcein present within endosomes is represented by punctate staining while calcein present in the cytoplasm is represented by diffuse staining (larger photograph shown on left). Intracellular PP75-AF647 staining is present almost exclusively in circular clusters and this is more consistent with pore formation within otherwise intact endosomes than complete rupture of endosomes (magnified views of inset shown on right). The scale bar represents 30 μm in the left side image and 2 μm in the right side images. (**D**) Cells were incubated with TMR-labeled dextrans (red fluorescence) ranging in size from 3kD to 70 kD. In the absence of PP75 (Ø), even the smallest tested dextrans remain localized within endosomes and are not visualized in the cytoplasm. In the presence of PP75 (+PP75), even the largest tested dextrans are released into the cytoplasm. The scale bar represents 20 μm.

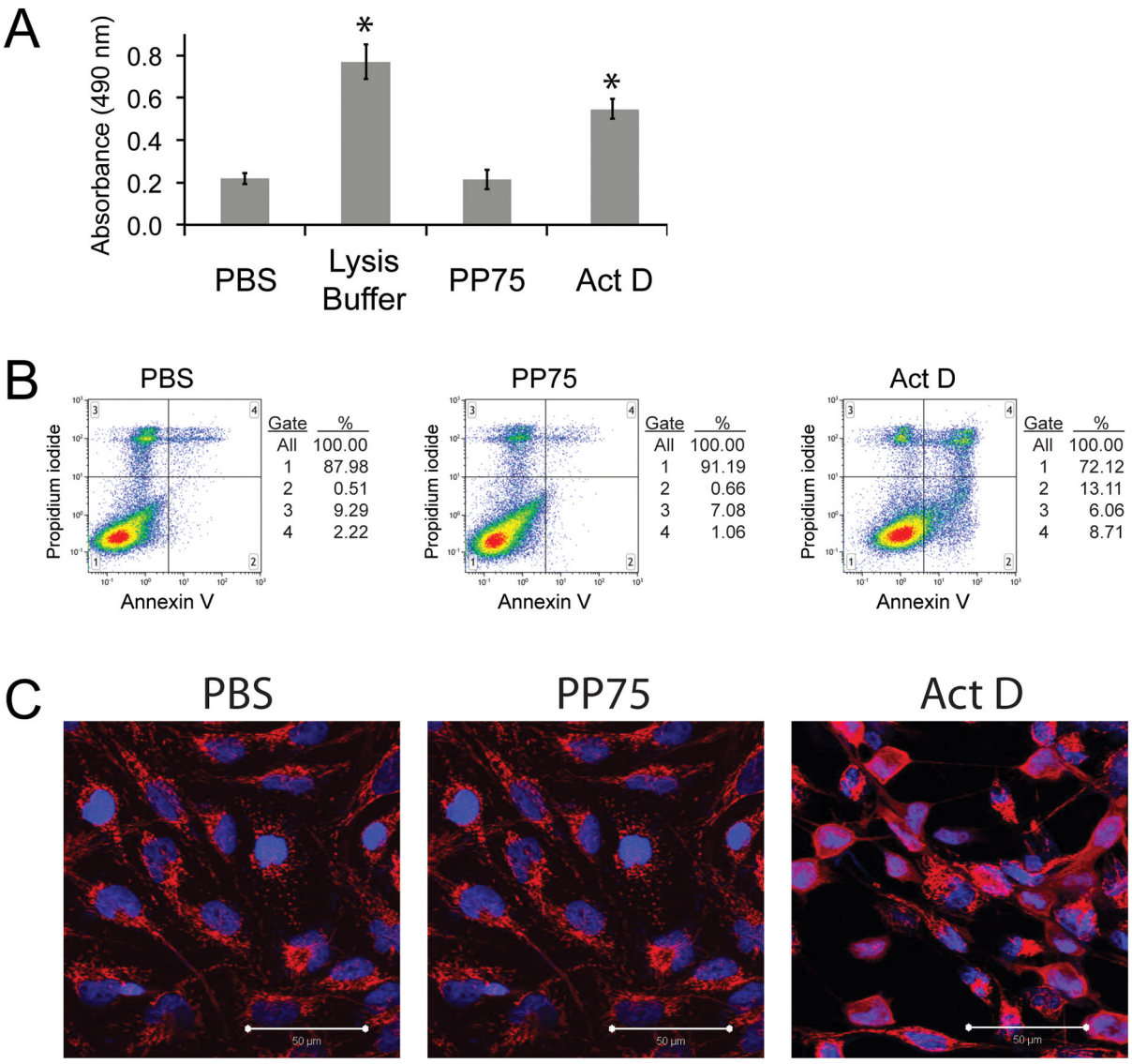

Fig. 3. Viability and apoptosis analyses

(A) Lactate dehydrogenase (LDH) release assay. Cells incubated with PBS control, a detergent cell lysis buffer, PP75 or actinomycin D (Act D – an apoptotic agent) were assessed for the release of cytoplasmic LDH into the culture medium. LDH in the culture medium was assessed by the addition of a substrate that is enzymatically converted to a product that absorbs 490 nm wavelength light (y-axis). Complete lysis of cells with detergent results in the relative maximal LDH release value. There is no significant difference in the amount of LDH released from PBS and PP75 treated cells. Asterisks indicate a significant difference in LDH release in comparison to PBS alone ($p < 0.05$; student's t test). **(B)** FACS analyses of PI and annexin V staining. Two color FACS histograms of cells incubated with PBS control, PP75 or Act D (a positive control) are shown. The y-axis represents the intensity of propidium iodide staining and is an indicator of plasma membrane compromise and/or cell death. The x-axis represents the labeling of cells with fluorescently tagged annexin V, which binds to apoptotic cells. There are no significant differences in the percentages of PI labeled cells (gates 3 and 4) or annexin V labeled cells (gates 2 and 4) in PBS and PP75 treated cell populations. In contrast, there is a large

increase in the percentage of PI and annexin V labeled cells in Act D treated cultures. Experiments were performed in triplicate and representative results are shown. **(C)** Cytochrome C staining. Cells treated with PBS control, Act D or PP75 were assessed for apoptosis by staining with anti-cytochrome C antibodies followed by red fluorescently labeled secondary antibodies. Cytochrome C is contained within mitochondria in healthy cells and displays a punctuate or granular staining pattern as seen in the PBS and PP75 treated cells. In cells undergoing apoptosis, cytochrome C is released into the cytoplasm and this results in a homogenous staining pattern as seen in the Act D treated cells. Cells were counterstained with DAPI to reveal cell nuclei (blue) and the scale bar in the lower right hand corner represents 50 μm.

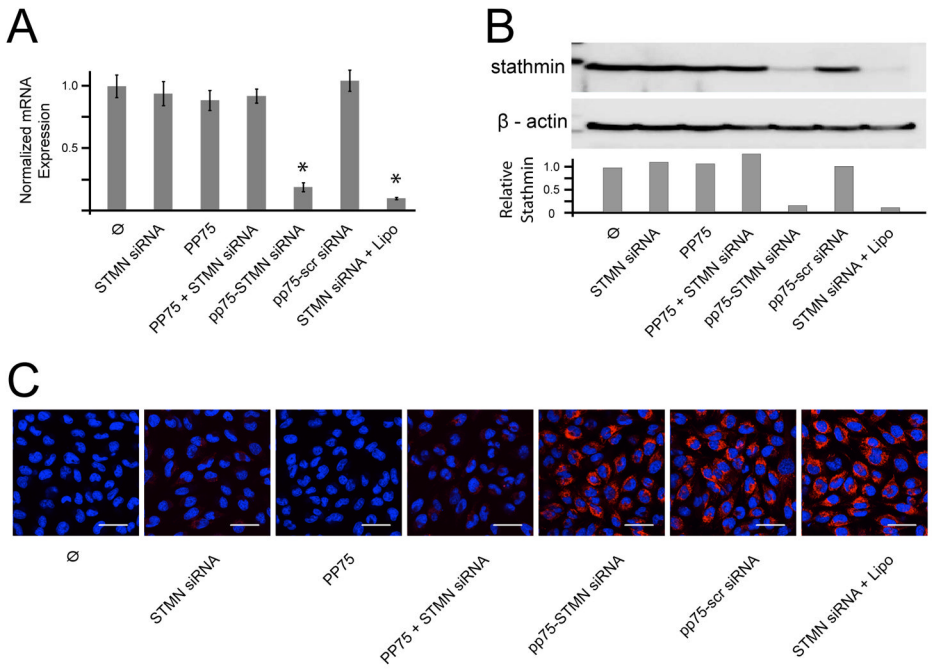

Fig. 4. PP75-stathmin siRNA delivery *in vitro*

(**A**) Relative stathmin mRNA expression levels for untreated control cells (Ø) and cells treated with stathmin siRNA alone (STMN siRNA), PP75 alone (PP75), PP75 plus stathmin siRNA without conjugation (PP75+STMN siRNA), PP75-stathmin siRNA conjugates (PP75-STMN siRNA), PP75-scrambled siRNA conjugates (PP75-scr siRNA) or stathmin siRNA plus Lipofectamine (STMN siRNA + Lipo). Values shown are the average of three experiments with error bars representing the standard deviation. Asterisks indicate $p < 0.002$ in comparison to untreated cells. (**B**) Stathmin protein expression for U251 cells treated as in Fig. 4A were determined by immunoblotting using an anti-stathmin antibody. Relative signal intensity of stathmin bands compared to β actin protein loading control bands are shown below the immunoblot image. Blots were performed in triplicate and representative results are shown. (**C**) Fluorescence microscopic visualization of U251 cells treated as in (A) except siRNAs were Cy3-labelled (red fluorescence). Nuclei are labeled with Hoechst 33342 (blue fluorescence). Experiments were performed in triplicate and representative views are shown. The white scale bars represent 50 μm.

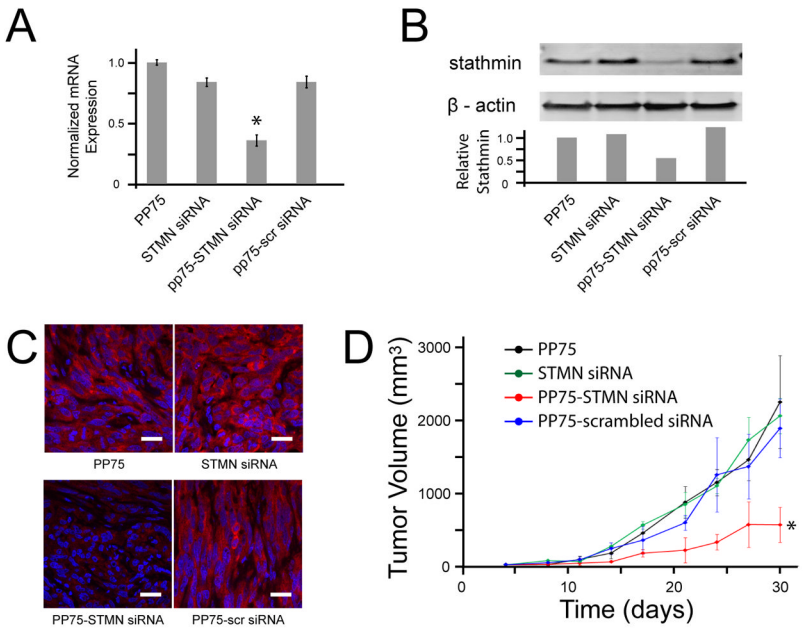

Fig. 5. PP75-stathmin siRNA delivery *in vivo*

Subcutaneous flank tumors were established by implantation of U251 cells into immunodeficient nude mice. On days 5 and 6 following the appearance of tumors, tumors were injected with PP75 alone (PP75), STMN siRNA alone (STMN siRNA), PP75-stathmin siRNA conjugates (PP75-STMN siRNA) or PP75-scrambled siRNA conjugates (PP75-scr siRNA). (**A**) Tumors were removed two days following treatment and relative stathmin mRNA expression levels were determined. The mean expression values of three tumors for each condition are shown. The error bars represent the standard deviation and the asterisk indicates $p < 0.005$ in comparison to PP75 treated tumors. (**B**) The tumors analyzed in fig. 5A were analyzed for stathmin protein expression by immunoblotting using an anti-stathmin antibody. Relative signal intensity of stathmin bands compared to β actin protein loading control bands are shown below the immunoblot image. Blots were performed in triplicate and representative results are shown. (**C**) The tumors analyzed in fig. 5A were also assessed for stathmin protein expression by immunohistochemistry using a primary rabbit anti-stathmin antibody and a fluorescently labeled anti-rabbit secondary antibody (red signal). Sections were counterstained with DAPI to reveal cell nuclei (blue). Representative sections from each treatment condition are shown and the scale bars correspond to 20 μm. **(D)** Two days following tumor treatment, animals not sacrificed for stathmin mRNA and protein expression analyses received intraperitoneal injection of the chemotherapeutic agent carmustine. Tumors were measured every 3 to 4 days and calculated mean volumes are shown with error bars representing standard deviations. PP75-STMN siRNA treated tumors significantly differ from each of the three control treated groups (*$p < 0.001$; two-way ANOVA).

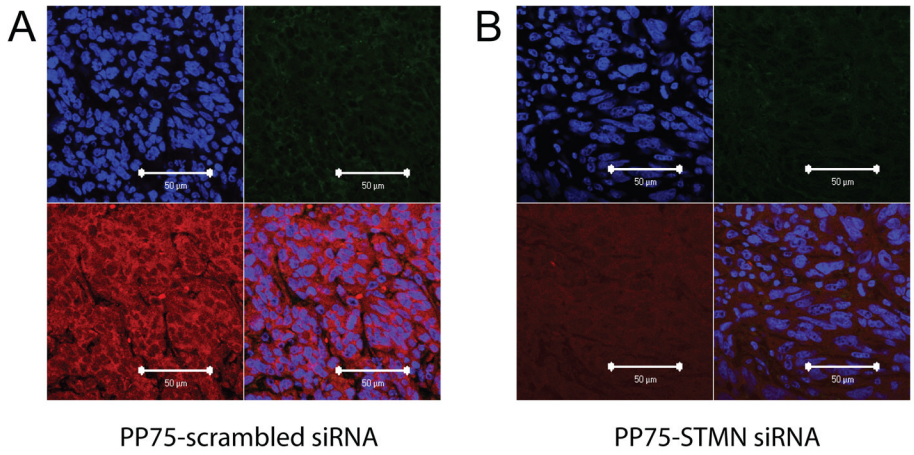

Fig 6. Assessment of immune infiltrates

Subcutaneous flank tumors injected withPP75-scr siRNA (A) or PP75-STMN siRNA (B) conjugates were harvested three days later and processed for immunohistochemical analyses. Tissue sections were counterstained with DAPI to reveal cell nuclei (upper left panels). The presence of immune cell infiltrates was assessed by staining with an anti-CD11b primary antibody followed by a green fluorescently labeled secondary antibody (upper right panels). Stathmin expression was assessed using an anti-stathmin primary antibody followed by a red fluorescently labeled secondary antibody (lower left panels). A merged photomicrograph of the upper left, upper right and lower left panels is shown in the lower right panels. The scale bar in the lower right corner of each panel represents 50 μm.